Photoluminescence Properties of the CdSe Quantum Dots Accompanied with Rotation of the Defocused Wide-Field Fluorescence Images

Qiang Li, Xiao-Jun Chen, Yi Xu, Sheng Lan, Hai-Ying Liu, Qiao-Feng Dai, and Li-Jun Wu*

Laboratory of Photonic Information Technology, School for Information and Optoelectronic Science and Engineering, South China Normal University, Guangzhou 510006, People's Republic of China

Received: January 23, 2010; Revised Manuscript Received: June 17, 2010

By tracking the dynamics of the emitting field of single CdSe/ZnS core−shell quantum dots (QDs), the defocused image (DI), i.e., emission pattern of some QDs was observed to rotate after blinking-*off* periods in our previous paper. To gain insight into this phenomenon, here we have extended the observation time to 350 s and traced the DIs of a number of individual QDs under different environments. It has been found that the "active" QDs (of which the DI changes) blink less frequently than the "normal" QDs and remain dark most of the observation time. Upon illumination in air, the occurrence probability of the DI rotation in the CdSe core QDs was observed to be as high as 18%. For those CdSe QDs passivated with ZnS shells, the occurrence probability dropped to 3%. When they were protected further by the PVA or PMMA film, the probability dropped to as low as ∼5‰. We propose that the surface defects of the QDs could form a type of carrier traps, which may influence the electron cloud and lead to a relatively high occurring probability of the "self-rotation" of the DI. Further, it seems that the surface defects could affect the recapture of the ejected carrier of the QDs and result in a longer mean *off*-time for the "active" QDs.

Introduction

Colloidal semiconductor quantum dots (QDs) with a diameter of a few nanometers present many attractive properties such as high photoluminescence (PL) quantum yield, tunable emission wavelength, exceptional photostability, multiplexing capabilities, and high photoresistance for chemical and potential biological applications.[1−3] The brightness and stability, however, are still two key parameters to determine their practical applications. Even under steady laser illumination, the PL of single QDs displays strong fluctuations, with dark periods or *off* times. This phenomenon called blinking is a hallmark of single fluorescent nano-objects.[4−8] It limits the brightness and visibility of QDs, and thus their potential applications.[9] The mechanism of blinking is still an open problem. The most popular model that describes blinking in single QDs was developed by Efros and Rosen,[10] in which the fluorescence intermittency of QDs is usually interpreted in terms of a photoinduced ionization process which leads to a charged QD. The free carrier in the QD can effectively quench the emission by a nonradiative Auger process. Later, a pronounced correlation between the fluorescence intermittency and large spectral shifting event was found. To explain the correlation between these two phenomena, a charge-reorganization model, which is extended from the photoionization model, was proposed.[11]

Recently, we employed the defocused imaging technique based on the wide-field fluorescence microscope to observe the space-distribution of the emitting field of single CdSe/ZnS core/shell QDs directly.[12] As this technique is based on the electron transition dipole approximation and the fact that the dipole radiation exhibits an angular anisotropy,[13] the spatial distribution of the emitting field (defocused image) and the deduced polarization characteristic therefore not only provides the information on the geometric structure symmetry of the single QD but also reflects the symmetry of the electron cloud (i.e., wave statistic function) in each QD.[14] By tracking the dynamics of the emitting field of single QDs, the defocused image (DI), i.e., emission pattern of some QDs was observed to rotate after blinking-*off* periods. We attributed this change as a "self-rotation" of the electron cloud around the "dark axis" (non-emitting axis) of the QDs. This is direct evidence not only for the photoionization model that describes blinking in semiconductor QDs but also for its extended charge-reorganization model that describes the correlation between blinking and large spectral shifting. However, our previous study was preliminary. More detailed investigations are necessary for understanding the physical mechanism underlying the observed phenomenon. On the basis of the previous results, we explore here the difference between the "active" QDs (of which the DI changes after blinking-*off* periods during the observation time) and "normal" QDs (of which the DI remains unchanged). It is found that the "active" QDs blink less frequently and remain dark most of the observation time. The occurrence probability of the "self-rotation" of DI depends on the immediate environment of the QDs. We propose that when the QDs are illuminated, oxygen in the immediate environments could corrode the surface of the core and induce surface defects, which could perform as a type of trap. The surface defect traps may influence the electron cloud and result in an easier occurrence of "self-rotation" of DI. In addition, the surface defect seems likely to affect the recapture of the ejected carrier and quench the emission of the QDs, which leads to a longer mean *off*-time for those QDs with DI rotation accompanied after blinking-*off* periods than those without. On the other hand, the irreversible photobleaching caused by the photooxidation of the QDs leads to a much faster drop of PL for the QDs (especially those without passivating shells) illuminated in air than in the polymethyl methacrylate (PMMA) or polyvinyl alcohol (PVA) film.

* To whom correspondence should be addressed. E-mail: ljwu@scnu.edu.cn.

10.1021/jp1006632
Published on Web 07/27/2010

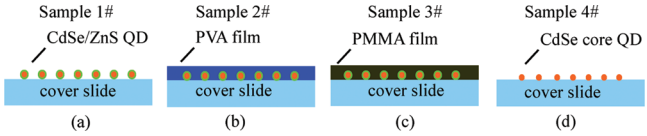

Figure 1. Schematic diagrams of four samples. QDs are fixed (a, d) between the slide (the refractive index $n = 1.458$) and air ($n = 1.0$), (b) between the slide ($n = 1.458$) and the PVA film ($n = 1.55$), and (c) between the slide and the PMMA film ($n = 1.5$), respectively.

Experimental Methods

As the immediate surroundings (local environment) are very important in determining the PL properties of QDs,[15,16] we fabricated four types of samples to provide different environments. The CdSe core and CdSe/ZnS core−shell QDs have been obtained from NNC Laboratories, of which the typical transmission electron microscopy (TEM) images, size distribution, absorption, and PL spectra can be found in Figure S1 (Supporting Information). Figure 1 depicts the schematic diagrams and the structural parameters of the samples. The detailed fabrication procedure for samples 1 and 4 are described in ref 12. The CdSe/ZnS core−shell and CdSe core QDs were uniformly distributed on the slides by capillary force. Sample 2 was obtained by spin-coating a ~200 nm thick PVA film on sample 1. For sample 3, the PVA film was substituted by the PMMA film. Through these procedures, four different environments for QDs were obtained, as shown in Figure 1.

The details for our experimental setup are similar to what are shown in ref 12. In short, the samples were excited by a diode-pumped solid-state laser (532 nm, 100 W/cm^2, Coherent) that is directed through a Zeiss 100×/1.4NA oil immersion objective. A half wave plate was inserted into the incident circuit to rotate the polarization of the excitation with respect to the laboratory reference system. Less than 10 mW of laser power was focused to a 20 μm diameter illumination spot on the sample substrate. With a long pass filter to block the excitation light in the detection path, the PL from QDs was collected by the same objective and detected with an intensified charge-coupled device (CCD) (Carl Zeiss) camera, as shown in Figure 2a. We adjusted the image focusing by stepwise moving the objective until we achieved diffraction-limited images of the QDs. Next, the position of the objective was moved by around −1.2 μm toward the sample for image defocusing. All the fluorescence images were recorded at room temperature. The raw data were collected in a series of consecutive images. The exposure time for each image was set to be 300 ms in order to obtain enough signal-to-noise ratio of the PL intensity. The analysis program then retrieves the intensity-time emission trajectories for all the chosen QDs, wherein each data point represents the averaged PL intensity in one selected area. The background intensity was determined locally around each monitored QD. The photostability measurement was conducted in a home-built grating spectrometer, through which the PL signal was continuously recorded by fixing the wavelength at 590 nm.

The program used to simulate DIs is based on the multidimensional dipole model developed by Enderlein and coworkers.[13,17] The orientation of the dipole system with respect to the laboratory system is sketched in Figure 2b. As shown, (X, Y, Z) and (x, y, z) indicate the coordinates of the laboratory and dipole systems, respectively. The Z axis is the optical axis. Three Euler angles (Ω, Ψ, ω) are defined to establish the relationship between them. Here we apply a modified 2D model with an elliptical parameter to describe the DIs of QDs[18] (Figure S2, Supporting Information). As can be seen, the orientation of the z-axis with regard to the lab system is determined by angles Ω and Ψ. The x and y directions are two "bright axes" for either symmetric or asymmetric structure.[13] The emissions along x and y axes are correlated in the modified 2D model and the z direction is the "dark axis" of the structure, which does not couple to the light field.[19]

Results and Discussion

To understand the underlying physics of the DI-rotating phenomenon in QDs, we extended the observation time to 350 s and traced the DIs of a number of individual QDs in four prepared samples. The time traces of the PL intensity and corresponding emission patterns of typical states with DI rotation from four representative "active" QDs (one example in each sample) are shown in Figure 3, which describes the phenomenology of blinking and emission pattern rotating during the tracing time. Parts a, b, c, and d of Figure 3 are the data from samples 1, 2, 3, and 4 respectively, in which the bottom panel is a magnified region of the time trace. Each data point represents one exposure. Figure 4 demonstrates the time traces of the PL intensity of four typical "normal" QDs (one example in each sample) without DI rotation observed during the tracking time. Comparing the results shown in Figures 3 and 4, the four "active" QDs appear to be emitting significantly less often than the four "normal" QDs and remain dark most of the time. The DI of the "active" QDs are shown in the insets of Figure 3a−d, in which the top images are the detected states and bottom the corresponding theoretical simulations. As we

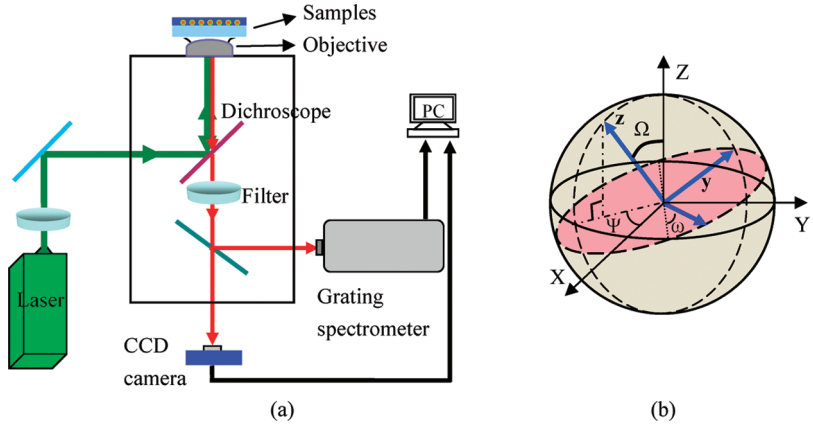

Figure 2. (a) Schematic of the defocused wide-field fluorescence imaging system. (b) Sketch of the simulation model to define the emission from a QD. The 3D orientation of the QD's reference system (x, y, z) with respect to the lab system (X, Y, Z) is determined by three angles Ω, Ψ, and ω.

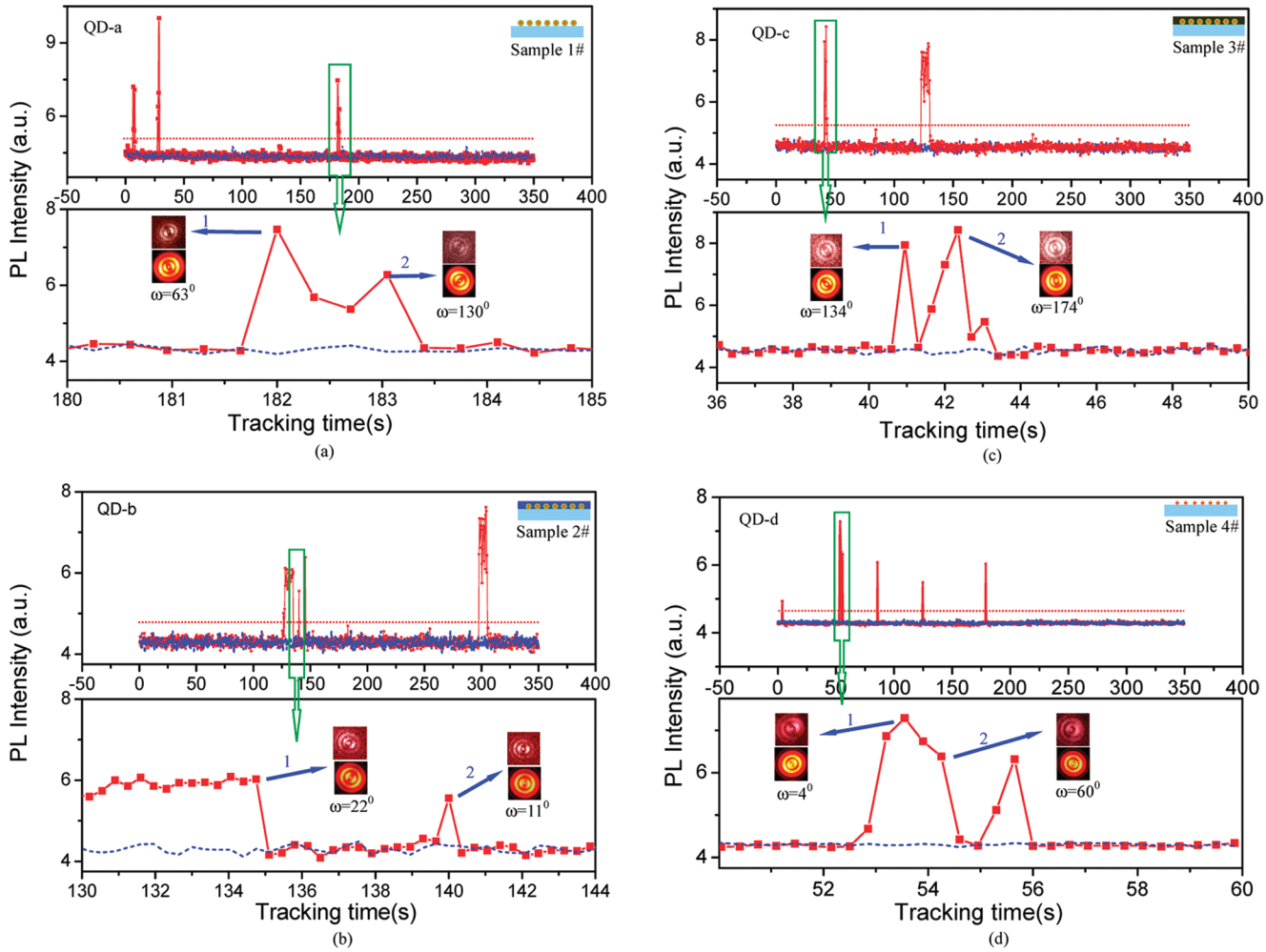

Figure 3. Time traces of the PL intensity of four representative "active" QDs: (a) for QD-a in sample 1, (b) for QD-b in sample 2, (c) for QD-c in sample 3, and (d) for QD-d in sample 4. Each dot corresponds to one exposure (300 ms). The blue dashed lines represent the local background obtained from the immediate surroundings of the monitored QDs. The bottom panel in parts a−d indicates a magnified region of the time trace, in which the inset plots the DI of some typical states for each monitored QD. In each group, the top image indicates the detected state and the bottom the simulated one. The thresholds to separate bright and dark periods are marked by the red dashed straight lines in the top panel.

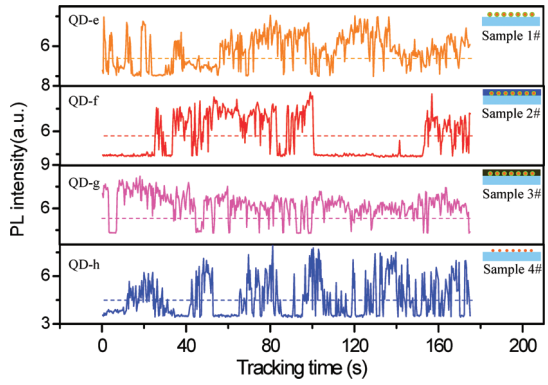

Figure 4. Time traces of the PL intensity of four "normal" QDs from four prepared samples. The insets sketch the configuration of the measured samples. The orange, red, magenta, and blue dashed lines mark the threshold to separate bright and dark periods.

have analyzed in our previous paper,[12] the temperature of the QD's environment is not close to its glassy transition temperature T_g and the "dark axis" determined by the crystal structure thus cannot rotate mechanically. Therefore, we can fix angles Ω and Ψ during the simulation as the "dark axis" is determined by Ω and Ψ (refer to Figure 2b). The change of ω, which represents the angle between the two coordinates (x, y) and (X, Y), is responsible for the rotation of DI. For example, during the tracking of QD-a as shown in Figure 3a, ω changes from 63° to 130° between states 1 and 2. It is worth noting that the signal with respect to the background is not so high although the exposure time was as long as 300 ms. We attribute this relatively low signal-to-noise ratio to the relatively low efficient detection of our apparatus and/or the long excitation wavelength (532 nm), which is close to the emission wavelength (598 nm). However, the signal demonstrated in Figures 3 and 4 can be clearly distinguished from the background and the DI-rotating phenomenon is apparent.

In principle, plotting both *on*-time and *off*-time probability distribution ($P(\tau_{on})$, $P(\tau_{off})$) enables us to extract the fluctuation dynamics of fluorescence intermittency. We traced the emission of 100 individual QDs and analyzed the data by means of a well-defined threshold, which separates bright and dark periods. Histograms for the duration of bright and dark periods were constructed for each individual QD and checked to be almost independent of the chosen threshold. Figure 5 summarizes the *on*-time and *off*-time probability distributions for 50 "normal" and 50 "active" QDs from sample 1. Although the probability distributions for the *on*-time and *off*-time depend on the chosen threshold value to

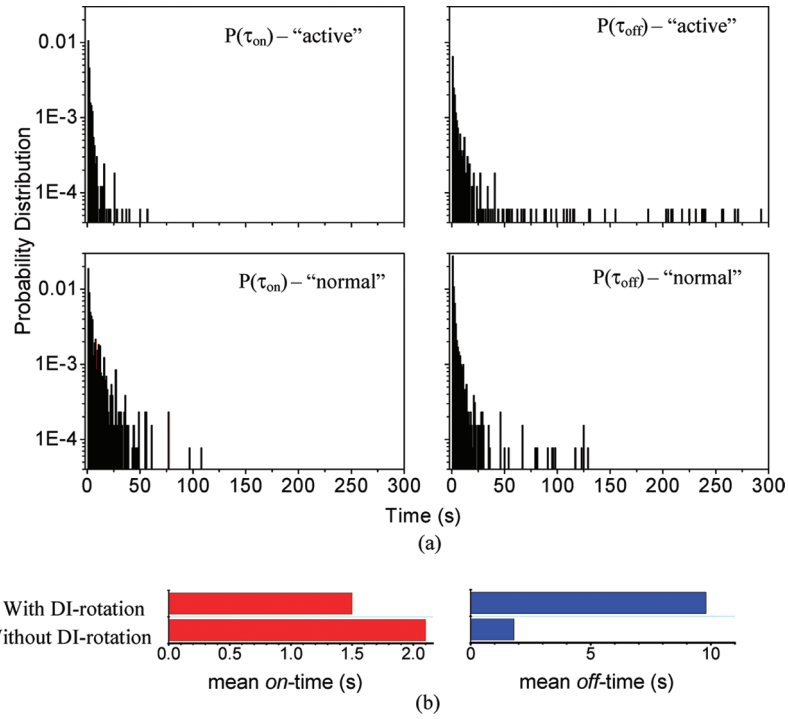

Figure 5. (a) Probability distributions of the *on*- and *off*-time for 50 "active" and 50 "normal" QDs in sample 1. (b) The mean *on*- and *off*-time for the two types of QDs.

separate bright and dark states in some degree which leads to an exponent spread,[20] the difference of $P(\tau_{on})$ and $P(\tau_{off})$ between the "active" and "normal" QDs is, however, too distinct to be influenced in our case. Obviously, both the *on*-time and *off*-time probability distributions of the "active" QDs are smaller than those of the "normal" ones when the time period is shorter than 50 s. When the time period is longer than 130 s, there are still considerable *off*-events for the "active" QDs whereas there are almost none for the "normal" QDs. These two phenomena indicate that the "active" QDs blink less frequently than the "normal" ones and they remain dark for longer periods. We can thus classify the blinking behaviors of the single QDs into two groups: (1) infrequent fluorescence blinking as shown in Figure 3 and (2) frequent fluorescence blinking as shown in Figure 4. To compare the difference between the "active" and "normal" QDs further, we calculated their mean *on*-time and mean *off*-time as in ref 21:

$$\text{mean} = \frac{\sum P(\Delta t)\cdot \Delta t}{\sum P(\Delta t)}$$

where Δt is the length of the *on*- or *off*-time and $P(\Delta t)$ is the appearance probability at Δt. As shown in Figure 5b, the mean *off*-time of the "active" QDs is obviously longer than that of the "normal" QDs by a factor of 4, indicating that the "active" QDs remain dark most of the observation time. The difference of the mean *on*-time between the "active" and "normal" QDs is, however, considerably small, suggesting that the distinction between them stems mainly from the *off*-periods.

As the environment influences the emission of QDs significantly,[15,16] we investigated the dependence of the occurring probability of the DI rotation on the immediate environments. By tracking the DI of 1500 single core−shell QDs in sample 1, it was found that more than 3% of them exhibited DI rotation. Nevertheless, the probability decreases to be at the order of magnitude of 5‰ in samples 2 and sample 3 when the core−shell QDs were protected by the PVA or PMMA film upon illumination. This decreasing trend led us to investigate the DI-rotating phenomenon in those QDs without passivating shells. It was found that more than 18% of these QDs exhibited DI rotation. We then monitored the fluorescence intensity of an ensemble of QDs as a function of time, as shown in Figure 6a. It is observed that the PL was considerably stable when the core−shell QDs were protected by the PVA or PMMA film even when the observation time was as long as 800 s. Upon illumination under air, only ∼42% of the PL left for the core−shell QDs and ∼10% left for the core QDs after 800 s. When we blocked the laser light periodically, the fluorescence intensity basically remained the same as its last value before the block from which it decreases again under light illumination, as shown by the black line in Figure 6b. From this result, we can deduce that the drop of the PL under air is irreversible.

The most likely reason for the decrease of the PL is due to photobleaching, which could be induced by the photochemistry reaction between the QDs and air.[16] Upon illumination in air, the surfaces of the CdSe core QDs are apt to be oxidized by oxygen, which leads to a fast drop of PL. When the surfaces of the CdSe QDs are passivated by ZnS shells, due to the lattice mismatch between the CdSe core and the passivating ZnS layer, the ZnS layer is not a closed epitaxial layer but rather a layer with grain boundaries. At these boundaries, oxygen can still diffuse to the CdSe core inside the ZnS shell upon illumination and induce photooxidation.[22] The main oxidation product was suggested to be SeO_2.[23,24] According to the conclusion from ref 16, 21, 25, and 26, the photooxidation of QDs influences their emission behavior significantly. During the process of photooxidation, photocorrosion may have taken place as the photobleaching shown in Figure 6b is irreversible.[16] Photocorrosion could create surface defects which likely enhance the nonra-

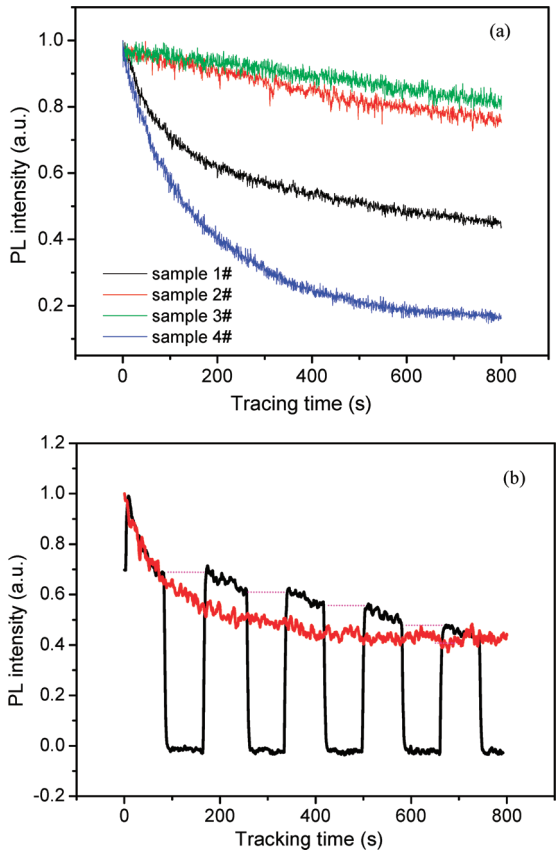

Figure 6. (a) Time traces of the PL intensity of ensemble CdSe/ZnS and CdSe core QDs under different environments. (b) Time traces of the PL intensity from the core−shell QDs recorded under air with constant illumination (red line) and periodic illumination (black line). The dashed magenta lines are guides to the eyes.

diative energy transfer in excited QDs and finally lead to irreversible photobleaching.[27]

As we have analyzed in our previous paper,[12] one possibility for the rotation of the DIs would be due to the change of the electron cloud around the "dark axis" of the QDs. The surface of QDs cannot only play an important role in determining their optical properties,[28,29] but it also influences their electron clouds. When the surface of the core is photocorroded, the generated surface defects could possibly influence the distribution of the electron cloud. Further, the defects are likely to be inhomogeneous on the surface of the QDs, the chance for the distribution of the electron cloud to be modified would be increased. During the illumination, the surface defects would be time-dependent whereby the electron cloud could possibly be modified continuously. As the surfaces of the CdSe core QDs without passivating shells are much easier to photocorrode by oxygen than those of the CdSe/ZnS core−shell QDs, its occurrence probability of DI rotation is remarkably larger upon illumination in air. When the core−shell QDs are protected by the PMMA or PVA film, the occurrence probability drops to ∼5‰ (it is not zero as the oxygen is still able to diffuse into the QDs through the poriferous PMMA or PVA film). One thing that needs to be noted is that not all the QDs show DI rotation before they are completely photobleached. These phenomena suggest that the activity of the DI rotation may be related to not only the number, but also the distribution of the surface defect traps. The distribution of the surface defects is likely to be related to the rate of photooxidation. When the photooxidation is very fast (such as in the case of the core QDs), the surface defects around the core of the QDs likely show large inhomogeneity and possibly result in a large occurrence probability of DI rotation. The quantitative analysis of the influence of the phtooxidation rate is still under investigation. Another interesting phenomenon we observed in the experiment is that the occurrence probability of DI rotation decreased with the illumination time. This could be possible because the "active" QDs are easier to photobleach than the "normal" ones and their number decreases faster.

The most popular model that describes blinking in semiconductor QDs was developed by Efros and Rosen,[10] which is called the photoionization model. They attribute the photoluminescence (PL) blinking to a random switching between emitting *on* and nonemitting *off* states due to the ionization of QDs under light excitation. When the QD is charged through Auger ionization, it becomes dark. The transition from a dark to a bright QD then occurs through recapture of the initial carrier back into the QD core or through capture of another carrier from nearby traps to neutralize the charged QD core. On the basis of this model, we assume that the surface defects could act as an additional class of trap states. One possibility would be that an Auger carrier is transferred from the core of the QD to the surface defect traps, thereby generating a charged QD. Neutralization of the QD might occur by recapture of the initial carrier back into the QD core or through capture of another carrier from nearby traps. With more surface defect traps, the chance for the trapped carrier to return to the core would be decreased and the dark periods of the QDs would be longer. Also the tunneling rate for recombination of an ejected charge carrier would be influenced by the surface defects. Obviously, the surface defect traps would influence the neutralization more significantly than the charging. Therefore, the mean *off*-time would be longer for those QDs with DI rotation (Figure 5b).

Conclusions

In summary, by tracking the QDs with/without the accompanying DI rotation phenomenon, we found that the "active" QDs blink less frequently than the "normal" QDs and remain *off* most of the observation time. Upon illumination in air, the occurrence probability of the DI rotation for the CdSe core QDs without passivating shells was as high as 18%. It dropped to ∼3% when the cores are passivated by the ZnS shells. The probability dropped further to as low as ∼5‰ when the core−shell QDs were protected by the PVA or PMMA film. We proposed that the surface defects could act as a kind of trap. These surface defect traps could influence the electron cloud and probably cause the DI to rotate. As the CdSe core QDs without passivating shells are much easier to photocorrode by oxygen than the CdSe/ZnS core−shell QDs upon illumination, the probability for DI rotation to occur would be much higher. Furthermore, the surface defect seems to be able to affect the recapture of the ejected carrier and quench the emission of the QDs, which result in a longer mean *off*-time for the "active" QDs. On the other hand, the photooxidation could cause an irreversible photobleaching of the QDs whereby the drop of the PL in air is much faster than that in the PMMA or PVA film.

Acknowledgment. The authors acknowledge the financial support from the National Natural Science Foundation of China (Grant Nos.10774050 and 10974060) and the Program for Innovative Research Team of Higher Education in Guangdong (Grant No. 06CXTD005).

Supporting Information Available: Figure S1showing typical TEM images of the CdSe/ZnS core-shell QDs investi-

gated, Size distribution of the QDs, and absorption and emission spectra of the QDs; details on the model used to simulate the defocused images of CdSe QDs; and Figure S2 showing the 3D orientation and corresponding calculated defocused image of different QDs with different Euler angles. This material is available free of charge via the Internet at http://pubs.acs.org.

References and Notes

(1) Efros, Al. L.; Rosen, M. The electronic structure of semiconductor nanocrystals. *Annu. Rev. Mater. Sci.* **2000**, *30*, 475–521.

(2) Medintz, I. L.; Uyeda, H. T.; Goldman, E. R.; Mattoussi, H. Quantum dot bioconjugates for imaging, labelling and sensing. *Nat. Mater.* **2005**, *4*, 435–446.

(3) Michalet, X.; Pinaud, F. F.; Bentolila, L. A.; Tsay, J. M.; Doose, S.; Li, J. J.; Sundaresan, G.; Wu, A. M.; Gambhir, S. S.; Weiss, S. Quantum dots for live cells, in vivo imaging, and diagnostics. *Science* **2005**, *307*, 538–544.

(4) Vanden Bout, D. A.; Wai-Tak, Y.; De-hong, H.; Dian-Kui, F.; Swager, T. M.; Barbara, P. F. Discrete Intensity Jumps and Intramolecular Electronic Energy Transfer in the Spectroscopy of Single Conjugated Polymer Molecules. *Science* **1997**, *277*, 1074–1077.

(5) Clifford, J. N.; Bell, T. D. M.; Tinnefeld, P.; Heilemann, M.; Melnikov, S. M.; Jun-ichi, H.; Sliwa, M.; Dedecker, P.; Sauer, M.; Hofkens, J.; Yeow, E. K. L. Fluorescence of Single Molecules in Polymer Films: Sensitivity of Blinking to Local Environment. *J. Phys. Chem. B* **2007**, *111*, 6987–6991.

(6) (a) Wang, S.; Querner, C.; Emmons, T.; Drndic, M.; Crouch, C. H. Fluorescence Blinking Statistics from CdSe Core and Core/Shell Nanorods. *J. Phys. Chem. B* **2006**, *110*, 23221–23227. (b) Kuno, M.; Fromm, D. P.; Hamann, H. F.; Gallagher, A.; Nesbitt, D. J. "On"/"off" fluorescence intermittency of single semiconductor quantum dots. *J. Chem. Phys.* **2001**, *115*, 1028–1040.

(7) Verberk, R.; van Oijen, A. M.; Orrit, M. Simple model for the power-law blinking of single semiconductor nanocrystals. *Phys. Rev. B* **2002**, *66*, 233202–233206.

(8) Frantsuzov, P.; Kuno, M.; Boldizs, Ã.; Jank, Ã.; Marcus, R. A. Universal emission intermittency in quantum dots, nanorods and nanowires. *Nat. Phys.* **2008**, *4*, 519–522.

(9) Heyes, C. D.; Kobitski, A. Y.; Breus, V. V.; Nienhaus, G. U. Effect of the shell on the blinking statistics of core-shell quantum dots: A single-particle fluorescence study. *Phys. Rev. B* **2007**, *75*, 125431–125439.

(10) Efros, A. L.; Rosen, M. Random Telegraph Signal in the Photoluminescence Intensity of a Single Quantum Dot. *Phys. Rev. Lett.* **1997**, *785*, 1110–1113.

(11) Neuhauser, R. G.; Shimizu, K. T.; Woo, W. K.; Empedocles, S. A.; Bawendi, M. G. Correlation between Fluorescence Intermittency and Spectral Diffusion in Single Semiconductor Quantum Dots. *Phys. Rev. Lett.* **2000**, *85*, 3301–3004.

(12) Chen, X.-J.; Xu, Yi.; Lan, S.; Dai, Q.-F.; Lin, X.-S.; Guo, Q.; Wu, L.-J. Rotation of defocused wide-field fluorescence images after blinking in single CdSe/ZnS core-shell quantum dots. *Phys. Rev. B.* **2009**, *79*, 115312–115318.

(13) Patra, D.; Gregor, I.; Enderlein, J.; Sauer, M. Defocused imaging of quantum-dot angular distribution of radiation. *Appl. Phys. Lett.* **2005**, *87*, 101103–101106.

(14) Hu, J. T.; Li, L. S.; Yang, W. D.; Manna, L.; Wang, L. W.; Alivisatos, A. P. Linearly Polarized Emission from Colloidal Semiconductor Quantum Rods. *Science.* **2001**, *292*, 2060–2063.

(15) Issac., A.; von Borczyskowski, C.; Cichos, F. Correlation between photoluminescence intermittency of CdSe quantum dots and self-trapped states in dielectric media. *Phys. Rev. B* **2005**, *71*, 161302–161306.

(16) Nazzal, A. Y.; Xiao-yong, W.; Min, X. Environmental Effects on Photoluminescence of Highly Luminescent CdSe and CdSe/ZnS Core/Shell Nanocrystals in Polymer Thin Films. *J. Phys. Chem. B* **2004**, *108*, 5507–5515.

(17) Böhmer, M.; Enderlein, J. Orientation imaging of single molecules by wide-field epifluorescence microscopy. *J. Opt. Soc. Am. B* **2003**, *20*, 554–559.

(18) Schuster, R.; Barth, M.; Gruber, A.; Cichos, F. Defocused wide field fluorescence imaging of single CdSe/ZnS quantum dots. *Chem. Phys. Lett.* **2005**, *413*, 280–283.

(19) Tittel, J.; Gohde, W.; Koberling, F.; Mews, A.; Kornowski, A.; Weller, H.; Eychmuller, A.; Basche, T.; Bunsenges, B. Investigations of the emission properties of single CdS-nanocrystallites. *Phys. Chem.* **1997**, *101*, 1626–1630.

(20) Frantsuzov, P. A.; Sa'ndor, V.-K.; Bolizsa'r, J. Model of Fluorescence Intermittency of Single Colloidal Semiconductor Quantum Dots Using Multiple Recombination Centers. *Phys. Rev. Lett.* **2009**, *103*, 207402–207406.

(21) Koberling, F.; Mews, A.; Basche, T. Oxygen-Induced Blinking of Single CdSe Nanocrystals. *Adv. Mater.* **2001**, *13*, 672–676.

(22) van Sark, W. G. J. H. M.; Frederix, P. L. T. M.; Van den Heuvel, D. J.; Gerritsen, H. C. Photooxidation and Photobleaching of Single CdSe/ZnS Quantum Dots Probed by Room-Temperature Time-Resolved Spectroscopy. *J. Phys. Chem. B.* **2001**, *105*, 8281–8284.

(23) Bowen Katari, J. E.; Colvin, V. L.; Alivisatos, A. P. X-ray Photoelectron Spectroscopy of CdSe Nanocrystals with Applications to Studies of the Nanocrystal Surface. *J. Phys. Chem.* **1994**, *98*, 4109–4117.

(24) Lee, S. F.; Osborne, M. A. Brightening, Blinking, Bluing and Bleaching in the Life of a Quantum Dot: Friend or Foe. *ChemPhysChem.* **2009**, *10*, 2174–2191.

(25) Cordero, S. R.; Carson, P. J.; Estabrook, R. A.; Strouse, G. F.; Buratto, S. K. Photo-Activated Luminescence of CdSe Quantum Dot Monolayers. *J. Phys. Chem. B* **2000**, *104*, 12137–12142.

(26) Nazzal, A. Y.; Lian-hua, Q.; Xiao-gang, P.; Min, X. Photoactivated CdSe Nanocrystals as Nanosensors for Gases. *Nano Lett.* **2003**, *3*, 819–822.

(27) Ma, J.; Chen, J.-Y.; Zhang, Y.; Wang, P.-N.; Guo, J.; Yang, W.-L.; Wang, C.-C. Photochemical Instability of Thiol-Capped CdTe Quantum Dots in Aqueous Solution and Living Cells: Process and Mechanism. *J. Phys. Chem. B* **2007**, *111*, 12012–12016.

(28) Gómez, D. E.; van Embden, J.; Jasieniak, J.; Smith, T. A.; Mulvaney, P. Blinking and Surface Chemistry of Single CdSe Nanocrystals. *Small* **2006**, *2*, 204–208.

(29) Gómez, D. E.; Califano, M.; Mulvaney, P. *Phys. Chem. Chem. Phys.* **2006**, *8*, 4989–5011.

JP1006632